hydrology

MDPI

Article

Evaluating country-scale irrigation demand through parsimonious agro-hydrological modeling

Nike Chiesa Turiano [1,2,*], Marta Tuninetti, Francesco Laio, Luca Ridolfi

ytechnic University of Turin
Correspondence: nike.chiesa@polito.it

Abstract

This study introduces WaterCROPv2, a state-of-the-art agro-hydrological model designed to estimate national-scale irrigation water demand while effectively balancing accuracy with practical data requirements. WaterCROPv2 incorporates innovative features such as hourly time-step computations, advanced rainwater canopy interception modeling, detailed soil-dependent leakage dynamics, and localized daily evapotranspiration patterns based on meteorological data. Through comprehensive analyses, WaterCROPv2 demonstrates significantly enhanced reliability in estimating irrigation water needs across various climatic regions, particularly under contrasting dry and wet conditions. Validation against independent data from the Italian National Institute of Statistics (ISTAT) for maize cultivation in Italy in 2010 confirms the model's accuracy and underscores its potential for broader international applications. Spatial analysis further reveals that estimation errors align closely with regional precipitation patterns: the model tends to slightly underestimate irrigation needs in wetter northern regions, whereas it somewhat overestimates demand in drier southern areas.Newly, WaterCROPv2 is here used to analyze irrigation water requirements for maize cultivation from 2005 to 2015, highlighting its significant potential as a strategic decision-support tool. The model identifies optimal cultivation areas, guides necessary crop transitions, and pinpoints regions where adopting efficient irrigation technologies could yield substantial water savings. Simulation results project that transitioning to micro-irrigation practices could reduce national water demand by 21%, with potential savings of 30–40% in historically water-rich areas with prevalent inefficient irrigation practices. The analysis emphasizes that regions currently lacking adequate irrigation infrastructure stand to gain the most from targeted irrigation system investments.

Keywords: Water Consumption; Irrigation; Agriculture; Remote Sensing

check for updates

Received:
Revised:
Accepted:
Published:

Citation: . . *Hydrology* **2025**, *1*, 0. https://doi.org/

Copyright: © 2025 by the authors. Licensee MDPI, Basel, Switzerland. This article is an open access article distributed under the terms and conditions of the Creative Commons Attribution (CC BY) license (https://creativecommons.org/licenses/by/4.0/).

Key points:

1. WaterCROPv2 is an advanced agro-hydrological model designed to estimate irrigation water demand at a national scale by effectively balancing hydrological accuracy with manageable data requirements.
2. The model aligns well with Italian National Institute of Statistics data for maize, demonstrating its reliability and adaptability for use in other countries' agricultural contexts.
3. Transitioning to micro-irrigation could reduce Italian water demand by 21%, with savings of 30-40% in regions with inefficient systems.

1. Introduction

Water governance operates at multiple levels, from international organizations down to local consortia [1]. This multi-level approach is essential to guarantee that water policies and laws ensure both (water-dependent) food and energy security without undermining environmental protection. [2,3]. In fact, nowadays, 40% of the world's food production comes from irrigated land which, despite accounting for only 18% of the global cultivated land [4], accounts for from 60% [5] to 70% of total freshwater withdrawals [6,7]. This pressure on freshwater bodies is expected to increase significantly mainly due to the world population growth [8], dietary changes towards more water-demanding food choices [9,10], and the need to buffer the increased vulnerability of cultivated lands to climate extremes [11]. Furthermore, future alterations of the hydrological cycle due to climate change [12–15] will likely impact the natural availability of freshwater resources, making effective water governance even more crucial [16]. This highlights the need for effective local water management even in water-rich areas where water exploitation has often been overlooked [17].

Under these conditions, there is an ongoing effort to improve national agricultural water management to reduce both the agriculture's vulnerability to climatic variability and the stress on freshwater bodies and the associated ecosystem [18–20]. Effective national water management has, in fact, the potential to regulate local water withdrawals from water bodies, preventing the regional excessive use of irrigation water and reducing crop losses due to water stress [21,22].

To this aim, accurately evaluating irrigation demands, along with other water uses, is essential for right water management and allocation [23]. Comprehensive national-scale evaluations of agricultural water use can provide pictures of the current water consumption across different regions. This helps identifying areas where structural and management improvements are needed, thus supporting decision making. Furthermore, reliable models can simulate various potential scenarios and predict the impact of different water management practices, providing valuable insights for investments and action plans.

In this context, agro-hydrological models are powerful decision-support tools for evaluating agricultural water requirements at various scales [17,24–27]. Numerous models have been developed over the years to this purpose, encompassing a wide range of modeling approaches, accuracy levels, and flexibility [28,29].

On one hand, highly complex models offer great accuracy and physical detail but are typically field-specific, computationally demanding, and require detailed input data that is often difficult to obtain [30]. Recent joint GIS implementations allow one to estimate irrigation water demands at regional scales but do not support scenario analysis and necessitate specialized users [31,32]. It follows that these models are applied at the field scale, but are hardly upscalable at regional and national scales.

On the other hand, simpler large-scale models are adopted for simulations at continental and global scales [33,34]. They require much less information than the previous class of models but may be too crude for agricultural water planning and management at the regional scale [35]: They often fail to account for variations in irrigation practices or soil diversity at the municipal scale, operate on a daily time scale, and approximate the modeling of the soil water balance.

In this framework, our aim is to propose a physically-based, agro-hydrological model that balances the complexity of detailed models with the lower data demand of large-scale models. Our model describes all the main hydrological processes that determine agricultural water demand but, at the same time, requires data typically available at municipal resolution rather than using coarse spatial resolution as typically done on regional and global models. These features make the model suitable for planning and managing water

resources at regional scale. The proposed model, WaterCROPv2, builds upon the model WaterCROPv1 [36] we introduced in 2015, and describes the key components of the soil-atmosphere-plant continuum (e.g., effective precipitation, leakage, evapotranspiration) as functions of soil properties, crop type, growth period, and land management. Compared to the previous version, several improvements are introduced starting from the hourly resolution that better captures the system dynamics. Furthermore, WaterCROPv2 also includes rainwater canopy interception, soil-dependent leakage dynamics, and the diurnal trend of evapotranspiration. Finally, it also considers the efficiency of the applied irrigation systems, thus evaluating not only the theoretical crop water demand, but also the actual water volumes that have to be conveyed to the fields.

To show the potential of the proposed model, we will (i) describe the physical processes considered and their modelling, (ii) show the typical WaterCROPv2 output, highlighting the advantages obtained with the updates in the crop water demand assessment, (iii) focus on the irrigated maize cultivation in Italy as an exemplifying case study. The case study allows us not only to show WaterCROPv2 reliability in assessing irrigation water demand but also to shed light on how the model can be used to analyse scenarios aimed at saving irrigation water and reducing the stress on freshwater resources.

The WaterCROPv2 model and required input data are described in Section 2. The model application to the specific case study of irrigated maize cultivation in Italy is reported in Section 3. Finally, in Section 4 some possible use of the proposed agro-hydrological model are discussed and conclusions drawn.

2. Model and Data

WaterCROPv2 is presented in Section 2.1 while Section 2.2 lists the required data to run WaterCROPv2.

2.1. WaterCROPv2 model

WaterCROPv2 is an agro-hydrological bucket model that simulates the crop and irrigation water demand during the growing season depending on soil, climate, crop, and irrigation system features. The bucket is designed as a single soil layer whose depth corresponds to the length of the plant roots Zn. As Zn elongates during the plant growth, the control volume of the storage changes its depth accordingly. The bucket not only stores water but also receives and releases hourly volumes of water. The fluxes entering the storage are (see Figure 1) the effective precipitation (P_{eff}) and the crop blue water demand (ET_b), while the exiting ones are the leakage (L) and the actual evapotranspiration (ET_a) also known as crop water demand. P_{eff} is the precipitation P decreased firstly of the volumes of drizzle water intercepted by the canopy, T, and secondly of the runoff R.

The mentioned inputs and output fluxes entail the temporal fluctuations in the water stored in the soil, namely the so-called soil water content, WC. The water balance equation for the soil layer reads

$$\frac{\mathrm{d}WC(t)}{\mathrm{d}t} = P(t) - T(P(t)) - R(WC(t)) - ET_a(WC(t)) - L(WC(t)) + ET_b(WC(t)) \quad (1)$$

where the soil water content is expressed in mm, time t in hours, and fluxes in mm/hour. It is important to note that, as will be further described later on, R, ET_a, T, L, and ET_b are functions of the soil water content. WC can span from $WC = 0$ mm to the soil water content at saturation WC_{sat}, whose magnitude depends on the soil type and the roots length Zn. Specific WC values play a crucial role in regulating the input/output fluxes (Figure 2):

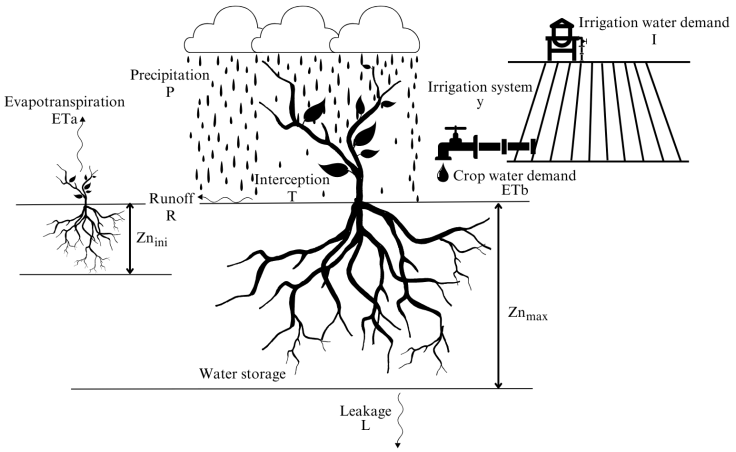

Figure 1. Water balance components of the bucket model: precipitation P, interception T, runoff R, evapotranspiration ET_a, crop water demand ET_b, and leakage L. Irrigation I is proportional to ET_b through an inefficiency factor dependent on the irrigation system y. The control volume expands together with the growth of the roots, Zn, from their initial length, Zn_{ini}, to their maximum one, Zn_{max}.

- WC_{wp}. It is the WC at wilting point and sets the minimum water content for plants to survive;
- WC_*. It is the WC at critical condition and it is the threshold that controls whether evapotranspiration is at maximum and whether it is necessary to resort to irrigation;
- WC_{fc}. It is the WC at field capacity and when WC goes below WC_{fc} the leakage process ends;
- WC_{sat}. It is the WC at saturation, which controls the surface runoff formation.

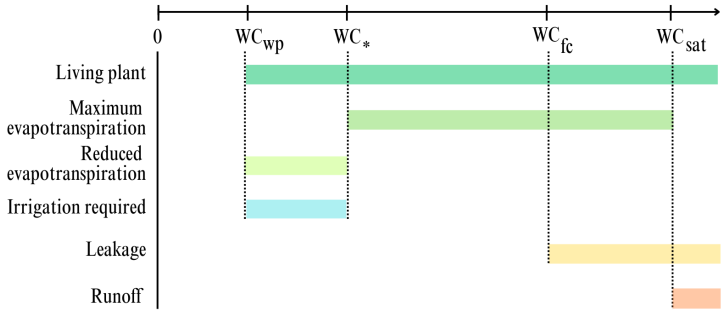

Figure 2. Ranges of possible water content (WC) values for different processes. Note that the light-blue bar of irrigation requirements shows the case of irrigation up to the critical level (WC_*).

The previously defined WC thresholds are not fixed values but are proportional to the length of the plant roots, Zn, that elongate during the growing season: the further the roots grow into humid soil, the larger becomes the amount of water (corresponding to the thresholds) contained in the control volume.

The growing period is subdivided into four growing stages, namely initial phase (establishment, lgp_1), development stage (vegetative, lgp_2), mid-season (flowering, lgp_3), and late season (yield formation and ripening, lgp_4). Taking Zn_{ini} as initial roots length, Zn_{max} as maximum length, and d as the day along the growing period, Zn is computed as [37]

$$Zn_t = \begin{cases} Zn_{ini} & \text{if } d = 1 \\ Zn_{ini} + \frac{Zn_{max} - Zn_{ini}}{lgp_1 + lgp_2} d & \text{if } d \in [lgp_1, lgp_2] \\ Zn_{max} & \text{if } d \in [lgp_3, lgp_4] \end{cases} \quad (2)$$

Zn is assumed to always be in the vadose zone. It follows that there is no interaction between root zone and the water table. For a visualization of the elongation trend of Zn during the growing period, refer to Figure F1 in Appendix F.

WaterCROPv2 is designed so that the continuous description of the water balance (Equation 1) in time t is discretized in hours that, every day, run from h=1 to h=24. This discretization implies that ET_a, L and P, which naturally occur during or throughout the whole day, are here hourly discretized. Every day, at the first hour, ($h = 1$ of the day d), the bucket stores the same volume of water as the last hour of the previous day, ($h = 24$ of day $d - 1$), plus ET_b, computed as the amount of water needed to reach the chosen water content, i.e. $WC_d(h = 1) = WC_{d-1}(h = 24) + ET_{b,d-1}$.

Evapotranspiration. ET_a takes into account plant transpiration and water evaporation from the soil. Each hour h along the growing period, ET_a is evaluated as

$$ET_a(h, d) = \begin{cases} ET_0(h, d) k_c(d) k_s(h) & \text{if } P(h) = 0 \\ 0 & \text{if } P(h) > 0 \end{cases} \quad (3)$$

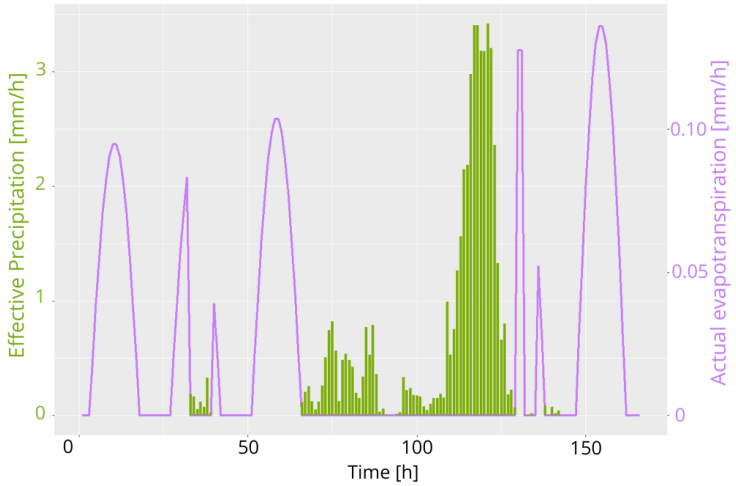

Figure 3. It is here reported the case of two rain events that stop the daily evapotranspiration process. The evapotranspiration behavior is shown for 6 days (from 28th to 35th day) in May of the initial stage of maize growth ($k_c \in$ [0.3-0.4125]) during which the plant is not under stress (k_s=1).

where ET_0 is the reference evapotranspiration, k_c is the crop coefficient, and k_s is the water stress coefficient. As ET_a rate is strongly driven by the gradient in relative humidity, Δe, between stomata and atmosphere, in case of rain events ($\Delta e \simeq 0$), ET_a is assumed to shut down.

ET_0 is defined as the evapotranspiration of a hypothetical well-watered grass reference crop with fixed height, albedo, and surface resistance [37]. Databases usually provide daily ET_0 values in spite of transpiration being a diurnal process that shows a peak around mid-day. In order to account for daily plant physiology, in WaterCROPv2, ET_0 is modelled according to [38]:

$$\begin{cases} ET_0(h,d) = \frac{ET_{0,d}(d)\pi \sin(\frac{\pi H}{N})}{2N} \\ N = ss - sr \\ H = h - sr \end{cases} \tag{4}$$

where $ET_{0,d}(d)$ is the daily evapotranspiration value corresponding to the day d, N is the amount of hours spanning from sunrise sr to sunset ss, H is the time elapsed since sunrise. Sunrise and sunset timing were defined, cell by cell, according to location (latitude and longitude) and day of the year.

The crop coefficient, k_c, is the coefficient that distinguishes the evapotranspiration rate of a specific crop from the one of the reference grass. k_c varies during the growing season depending on the crop development in order to take into account changes of crop height and leaf areas. In particular, k_c evolves in time as [37]

$$k_{c,t} = \begin{cases} k_{c,ini} & \text{if } d \in lgp_1 \\ \frac{k_{c,mid} - k_{c,ini}}{d - lgp_2} d & \text{if } d \in lgp_2 \\ k_{c,mid} & \text{if } d \in lgp_3 \\ \frac{k_{c,fin} - k_{c,mid}}{d - lgp_1 - lgp_2 - lgp_3} d & \text{if } d \in lgp_4 \end{cases} \tag{5}$$

where $k_{c,ini}$, $k_{c,mid}$, $k_{c,fin}$ are k_c at initial, mid, and final growing stages respectively, and d is the day along the growing period. Note that k_c values and lgps lengths depend on climate zone and crop type [37].

The water stress coefficient, $k_s \in [0,1]$ is the coefficient that specifies whether the plant is watered enough to evapotranspire at its potential. Thus, it is regulated by WC as [37]

$$k_s(h) = \begin{cases} 0 & \text{if } WC \leq WC_{wp} \\ \frac{WC(h) - WC_{wp}}{WC_* - WC_{wp}} & \text{if } WC \in [WC_{wp}, WC_*] \\ 1 & \text{if } WC \geq WC_* \end{cases} \tag{6}$$

To have a visualization of k_c trend during the growing period and of k_s trend as function of WC, please, refer to Figure F1 and F2, respectively, in Appendix F.

If soil water content is above the critical value, WC_*, the plant is in stress-free conditions and it evapotranspires at its maximum potential, $ET_a = ET_c$. Instead, whenever the water content is below the critical value the plant is under stress and the evapotranspiration is lower than the potential one, $ET_a < ET_c$. This linear reduction is due to a gradual closure of the stomata that results in a progressive diminution in water uptake. If wilting point is reached, $WC = WC_{wp}$, water uptake stops and evapotranspiration ceases, $ET_a = 0$. Physical evaporation can take place below wilting point, independently from plant transpiration. However, this phenomenon is not modeled here as this study focuses on irrigated crops that unlikely reach such conditions. Figure 3 reports an example of ET_a evolution (purple line): the last hump shows the undisturbed daily trend, while the previous humps point out the effect of rain (green bins). Rain events cause the interruption of daily ET_a but if the rain-water has time to evaporate from the leaves, ET_a kicks in again (second hump).

Leakage. Leakage is modelled with the following exponential law [39]

$$L(s) = \begin{cases} \frac{K_s}{e^{\beta(1-s_{fc})}-1}[e^{\beta(s-s_{fc})} - 1] & \text{if } s_{fc} < s \leq 1 \\ 0 & \text{if } s < s_{fc} \end{cases} \quad (7)$$

where K_s is the saturated hydraulic conductivity, β a soil-dependent coefficient, s the relative soil moisture defined as $s = WC/WC_{sat}$, and s_{fc} the relative soil moisture at field capacity. Coherently with the time discretization of water balance (Equation 1), L is evaluated with hourly steps.

Precipitation, interception, and runoff. To avoid very small precipitation values that do not affect the soil hydrological balance but, instead, can introduce spurious noise in the system dynamics, a filter was introduced: a rainfall is considered a rain event only if it accumulates at least 0.01 mm/h. Canopy interception, $T(h)$, is included by subtracting, from each rain event, 0.5 mm for grasses and 2 mm for trees [39]. Another key point is when rainfalls can be considered as two separate rain events. In this work, a reasonable break between two subsequent events was set at 5 hours.

Runoff, $R(h)$, is formed only if the effective precipitation, $P_{eff} = P(h) - T(h)$, brings in the control volume more water than the amount that can be stored. The overflowing water forms runoff as

$$\begin{cases} R(h) = P(h) - T(h) - WC_{av}(h) & \text{if } P_{eff} > WC_{av} \\ WC_{av}(h) = WC_{sat}(d) - WC(h) \end{cases} \quad (8)$$

Irrigation. WaterCROPv2 computes irrigation volumes I in two steps: first, it computes the crop blue water demand, ET_b, and secondly the irrigation volumes I (called irrigation water demand). ET_b corresponds to the theoretical amount of water needed to keep the soil at a chosen water content threshold, WC_{th}, taking into account soil dynamics (leakage) and plant physiology (evapotranspiration). Generally, WC_{th} is chosen so that the plant can evapotranspire at its potential: e.g. $WC_* < WC_{th} < WC_{FC}$. In WaterCROPv2 ET_b is applied - conventionally at $h = 24$ (but other choices are easily implementable) - only if the soil water content is below the chosen water content, and only to reach such threshold. It follows:

$$ET_b(d) = \frac{WC_{th}(d) - WC(h = 24)}{\Delta h} \quad (9)$$

Irrigation water demand I is the actual amount of water that the farmer has to provide to the field. Such value depends on the irrigation systems as it encloses the irrigation system inefficiency. There are several ways of defining the irrigation system inefficiency α according to the application [5]. In this work, we neglect the inefficiency of the conveyance system that transports water from the water body to the field, as we rather focus on the irrigation method present on the field (e.g. submersion, flow irrigation, sprinklers, micro-irrigation). Thus, in this work the irrigation inefficiency α ($\alpha > 1$) is defined, for each irrigation system, as the average ratio between the volumes of water provided to the field (I) and the one that has to infiltrate in the rootzone (ET_b), namely

$$I(d) = \alpha ET_b(d) \quad (10)$$

2.2. Data

WaterCROPv2 works at hourly temporal resolution on grid cells whose size is determined by the input data resolution. All the required data must be homogenized at the same spatial and temporal resolution. The required input data fall into four categories: crop data, soil data, climate data, and irrigation data.

Crop data. Crop data characterize the crop in terms of growth and response to water stress. They are: (i) daily reference evapotranspiration (ET_0, d), (ii) crop-specific growth coefficients (kc_{ini}, kc_{mid}, kc_{fin}), (iii) length of the four growing period stages (lgp_1, lgp_2, lgp_3, lgp_4), (iv) critical soil moisture (WC_*), (v) initial and maximum roots depth (Zn_{ini}, Zn_{max}), (vi) sowing and harvesting dates, and (vii) extension of irrigated areas. Notice that sowing and harvesting dates, length of the growing stages, and root depth depend on cultural conditions and on the local climate zone.

It is noteworthy that, in literature, it is easier to retrieve values of critical depletion fraction, Dr_*, rather than WC_*. Dr_* is defined as the critical soil water shortage with respect to field capacity and it is related to WC_* as follows

$$Dr_* = WC_{fc} - WC_* \tag{11}$$

Soil data. The description of runoff and leakage processes requires: (i) saturated hydraulic conductivity (K_s), (ii) volumetric water content at field capacity (θ_{fc}), (iii) volumetric water content at saturation (θ_{sat}), and (iv) the fitting coefficient (β). Note that the volumetric water content θ is defined as the ratio of water volume WC to soil volume V_{soil} (e.g. $\theta_{fc} = WC_{fc}/V_{soil}$).

Climate data. Major players in plants phenology are local climate and precipitation. Thus, (i) climate zone, (ii) hourly precipitation time-series, and (iii) geographical coordinates have to be provided for the studied area.

Irrigation data. WaterCROPv2 determines the irrigation water demand, I, from the blue water demand, ET_b (Equation 9). To do so the inefficiency factor α of the used irrigation systems has to be provided.

3. Results

WaterCROPv2 was developed to evaluate in a reliable and functional way irrigation water demand at seasonal and regional scale. As an example case we here report and analyse the outputs of the employment of WaterCROPv2 at the Italian national scale. In Section 3.1, firstly, maize irrigation demand obtained by WaterCROPv2 is compared to the evaluation obtained from the previous version WaterCROPv1 to show the effect of modeling improvements; secondly, the model reliability is assessed using independent data of irrigation water provided by the Italian national institute of statistics [40]. Lastly, Section 3.2 shows some possible applications of WaterCROPv2 model as decision-making tool using country-scale mean results for maize cultivation in Italy: maize is, in fact, one of the most water-demanding crops and, in Italy, it is so widely spread that alone accounts for more than 20% of the irrigated cropland [40]. Refer to Appendix E for an overview of the used data and the pre-processing employed to run WaterCROPv1 and WaterCROPv2 for the above mentioned analyses.

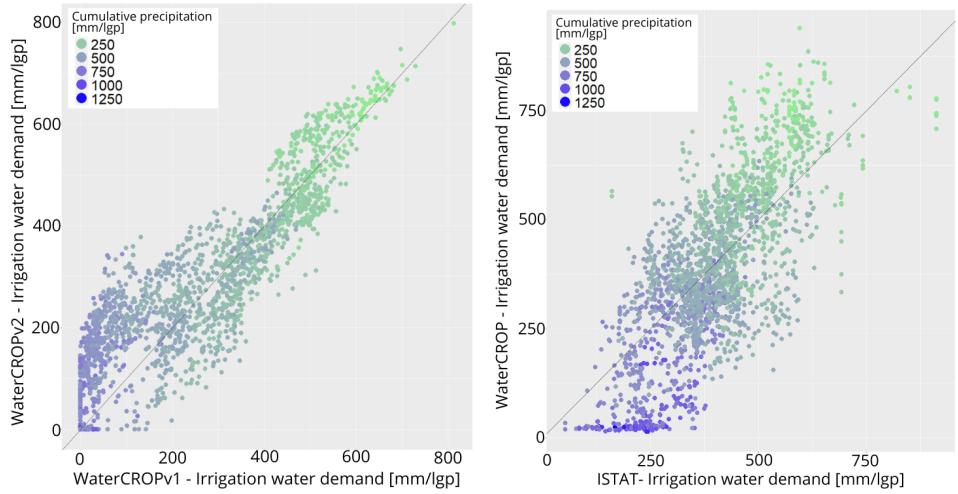

(**a**) (**b**)

Figure 4. Scatter plots comparing, cell by cell, the irrigation water demand of maize in 2010 in Italy computed by (a) WaterCROPv2 and WaterCROPv1 and (b) WaterCROPv2 and ISTAT database. The black line corresponds to the bisector. The color of the dots varies gradually from green (scarce precipitation) to blue (abundant precipitation) according to the values of cumulative precipitation over the growing season in the cell.

3.1. Validation

To analyze the impact of the updates introduced in version 2 both WaterCROPv1 and WaterCROPv2 were run with the same crop and irrigation data. The used data - provided by "Agricultural Census" [40] (Table E1 in Appendix E) - refer to maize cultivation in Italy in 2010.

The comparison was run analyzing the maize irrigation water demand (I_{mz}), defined as the cumulative sum of the daily volume required to keep the soil above a chosen water content, WC_{th}, over the growing period. In this case, WC_{th} was set to critical level WC_*. In Figure 4(**a**), the scatterplot compares WaterCROPv1 and WaterCROPv2 cell by cell. The two versions display general consistency, as the points tend to align along the bisector. However, relevant differences due to the modeling improvements emerge clearly. In particular, it is visible how the relative importance of the newly added processes (leakage and the shutting down of the evapotranspiration process), and the use of hourly precipitation time series play a major role in the differences of the versions. In fact, the dots' distribution exhibits a smaller dispersion for higher irrigation water values, a condition corresponding to a reduced relevance of the added physical processes: high irrigation demands are due to low precipitations, that only rarely trigger leakage and evapotranspiration shutting down. On the contrary, v1 and v2 show weaker correlations for lower water demand values, which correspond to high precipitation levels, when leakage and shutting down play a relevant role. Finally, notice the significantly lower number of zero irrigation water demands according to the improved model. This result demonstrates the importance of describing precipitation on an hourly scale rather than distributing monthly values uniformly. This allows capturing periods of water shortage even in regions characterized by high mean monthly precipitation.

In Figure 4(**b**) we tested WaterCROPv2 consistency with irrigation values provided by the Italian National Institute of Statistics [40]. In this case, I_{mz} values given by WaterCROPv2 correspond to the case of irrigation up to field capacity (WC_{th}=WC_{fc}), rather than to critical point: it is indeed of common practice, among the farmers, to irrigate up to field capacity.

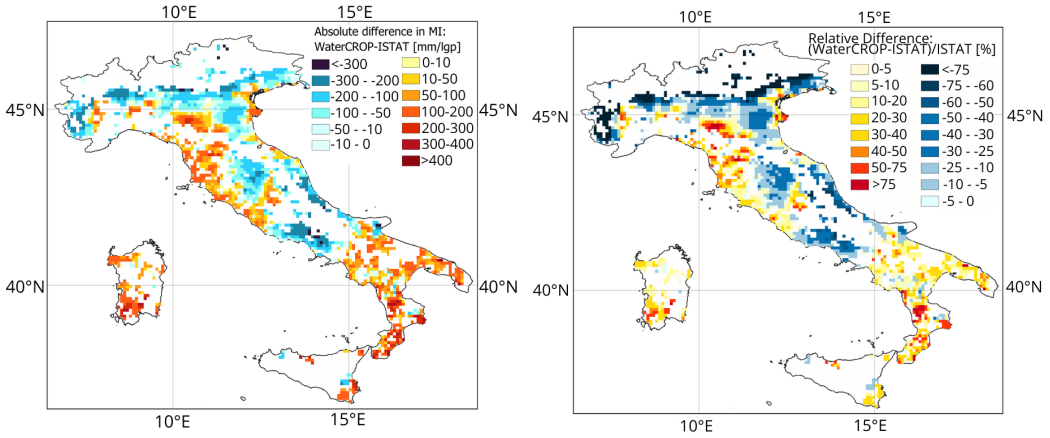

(**a**) (**b**)

Figure 5. (a) Absolute and (b) relative differences in irrigation water demand of maize in 2010 computed by WaterCROPv2 and ISTAT.

ISTAT values, instead, provided for each municipality, correspond to the output of the MARSALa model [41]: a model calibrated over 300 farms assumed to be representative of Italian agriculture. MARSALa is a more detailed and computationally demanding model with respect to WaterCROPv2 as it includes a section of irrigation method scheduling that requires additional input data. Furthermore, the model relayed on farm-level input data on sowing and harvesting dates, as well as on locally employed irrigation systems: none of which available in the "Agricultural Census" [40] database used to run WaterCROPv2. Due to the robustness of the source of the input data used to run MARSALa, we assume the output values as the benchmark for the evaluation of WaterCROPv2 reliability. Due to the different complexity of the irrigation models and the accuracy of input data, WaterCROPv2 values are not expected to precisely match ISTAT values but rather to exhibit a similar trend. Figure 4(**b**) confirms this expectation as dots align along the bisector. The observed relation between estimation errors and precipitation suggests a spatial distribution of the differences, which is confirmed in Figure 5(**a**)-5(**b**). Northern Italy, generally wetter (most of blue dots in Figure 4(**b**), shows a mean underestimation of 23% while, on the contrary, Southern Italy, generally drier (generally green dots in 4(**b**)), experiences a mean overestimation of 14%. Central Italy, with locally variable differences, shows a more consistent mean and distribution with a mean underestimation of 2%. The overestimation of WaterCROP2 can find a possible explanation in the fact that, especially in dry areas, it might be hard for the farmers to always irrigate up to field capacity meeting the model assumption. Lastly, note the dots in the bottom left of Figure 4(**b**), where WaterCROPv2 and ISTAT dataset show strong disagreement: they correspond to cells with high precipitation, mainly clustered in two specific pre-alpine areas in the North-West and North-East of the Italy. The real ground slope in those areas might explain the disagreement. In fact, runoff in sloped fields is generally larger than the one for flat areas: as WaterCROPv2 does not include a terrain model, the underestimation of the runoff in those areas, and the consequent infiltration overestimation, might result in smaller I_{mz} values.

3.2. Examples of model application

In this section, we present some possible applications of WaterCROPv2 as a tool to evaluate the irrigation water demand both in current state and scenarios of interest.
We used WaterCROPv2 to assess the mean present state of maize irrigation water demand (I_{mz}) in Italy. To do so, we forced the model with crop, soil, climate and irrigation data as specified in Appendix E and assumed an irrigation threshold up to critical level

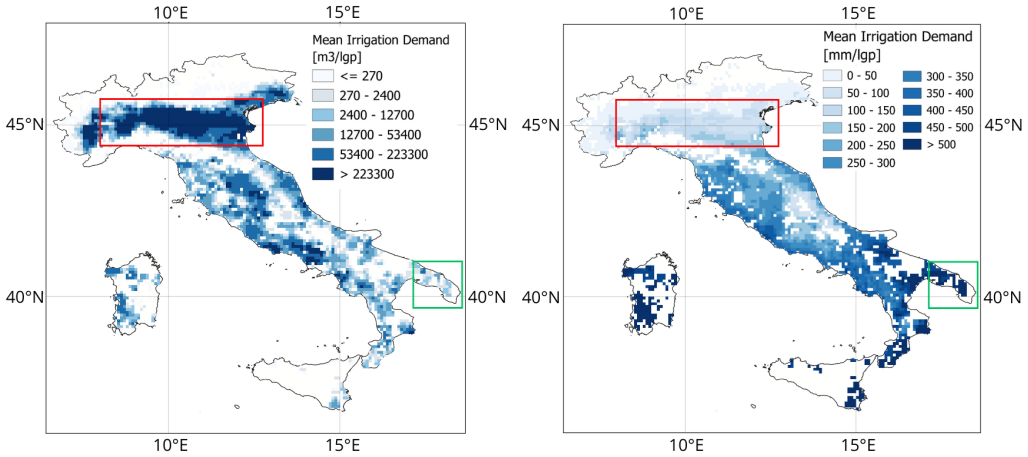

(**a**) (**b**)

Figure 6. Map of mean irrigation demand by maize in Italy expressed in (a) cubic meters, (b) millimeters. The red rectangle spotlights the Pianura Padana region, an area climatically suitable for maize cultivation but highly water-demanding; the green rectangle encloses the Salentino region, zone where the unfavourable climate discourages the maize cultivation resulting in small water-demand.

(WC_{th}=WC_*). The used precipitation record covers the period from 2005 to 2015 as this timespan is considered representative of the Italian climate. In fact, Italy in those years experienced fairly large oscillations in cumulative precipitation with dry (e.g. 2010-2011) and wet seasons (e.g. 2006-2007) [42]. The mean present state was evaluated by averaging the I_{mz} values for each simulated year. As defined in Equation E3, the mean I_{mz} is defined as maize blue water demand (ET_b) divided by weighted irrigation systems efficiencies. For each cell, the weight of each irrigation system is based on the relative number of hectares irrigated with that system with respect to the total amount of irrigated hectares. Figure 6(**a**) and Figure 6(**b**) show I_{mz} in cubic meters and millimeters, respectively, presenting two different perspectives. The cubic meters perspective reveals the total, actual amount of water used for maize in a specific cell. However, it does not provide information on the areal density of such amount of water. The millimeters, instead, corresponding to the normalization of the m^3 over the cultivated areas, provide this detail. Millimeters highlight which areas are more suitable for maize cultivation due to the local climate. The evident gradient in mm-demand from the wetter north to the drier south points out how the local climate strongly influences the water demand. Two good examples are Pianura Padana (red rectangle) and Salentino (green rectangle). In Pianura Padana, climate and soil are suitable for maize growth, with I_{mz} generally below 120 mm/lgp, leading to a large maize cultivation and high volumetric water demand (above 200,000 m^3/lgp). In contrast, Salentino area has a much drier climate, resulting in high mm-demand and less extensive maize cultivation, thus leading to a lower m^3 demand. It is noteworthy that most areas with the highest I_{mz} correspond to regions where maize is the primary crop (Figure E1(**a**), Appendix E), making maize the pivotal crop in those areas. The areas showing high or small water demand in both maps are areas the attention of decision-makers should be driven to. In fact, dark-blue cells in both maps are regions where the present extensive cultivation is actually located in areas poor in rainwater, and thus crop shifts should be put in place, light-grey cells, instead, spotlight zones where maize cultivation should be developed (focusing only on the maize perspective) as is not yet largely present despite favorable climate.

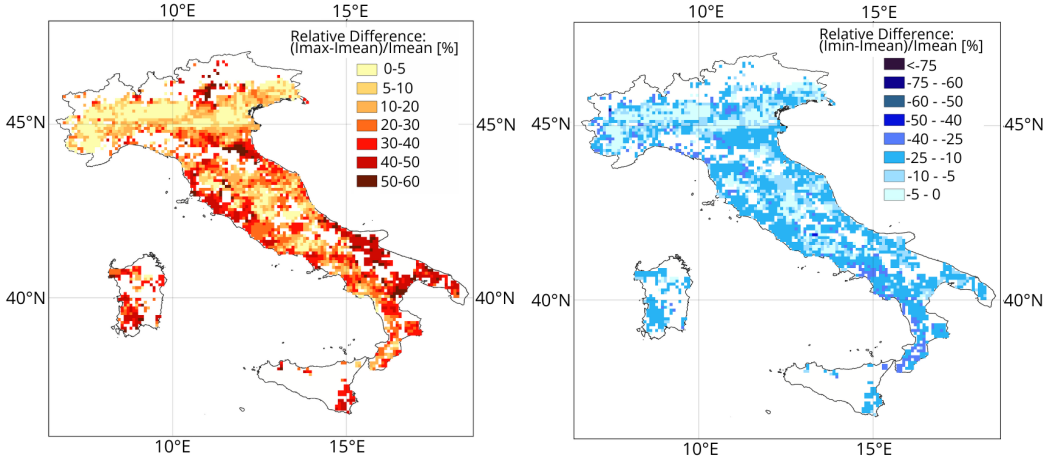

(**a**) (**b**)

Figure 7. Relative difference of (a) maximum and (b) minimum irrigation water demand with respect to the mean irrigation requirement.

The key sources of uncertainty, cell by cell, in the I_{mz} evaluation are the irrigation system heterogeneity and their efficiencies. While it is not possible to assess a range of local efficiencies in the absence of more information, instead a reasonable computation of the uncertainty in I_{mz} due to the heterogeneity and the relative relevance of the irrigation systems can be carried out. To the purpose, other two possible values of α were considered: respectively they correspond to the scenarios of upper (lower efficiency) and lower (higher efficiency) boundaries of I_{mz}. They can be defined based on whether maize was assumed to be irrigated primarily using less or more efficient irrigation systems: the upper α value was computed covering the irrigated area from the least efficient irrigation system to the most efficient one until exhaustion. For the lower α value, the irrigation systems were applied from the most efficient to the least efficient. Figures 7(**a**) and 7(**b**) display the offsets of the highest and lowest I_{mz} values, respectively as percentage deviations with respect to mean values. The correspondence of zones with the smallest deviations - [0-5%]: light yellow for the upper limit and light blue for the lower limit - among the figures indicate higher reliability of I_{mz} values, due to a smaller heterogeneity of irrigation systems in those areas. These cells account for almost 15% of the cells. In the majority of the cells (92%), the lower I_{mz} deviates less than 25% from the mean, while in 67% of cells the higher I_{mz} is at most 30% larger than the mean. This skewness of distribution around the mean is due to the fact that micro-irrigation, the most efficient system, covers less than 18% of the irrigated areas while flow irrigation, one of the least efficient methods, is used on over 30% (Table 1). If local information on the applied irrigation system were available, the uncertainty would be limited to the irrigation efficiency values, whose uncertainty has a smaller impact on I_{mz} computation at the national level.

4. Discussion and Conclusions

A key use of agro-hydrological models, such as WaterCROPv2, is to evaluate irrigation water demand. However, even though they are generally used as assessment tools, they can also be applied as modeling tools. In this sense, they are key instrument to analyze scenarios and propose alternatives to the current state. For instance, it is possible to analyze the effect of changing irrigation thresholds (e.g. irrigation up to fractions of field capacity) or timing (e.g. biweekly, weekly), to study the impact of different irrigation systems and to

investigate the effects of climate change. These scenarios are fundamental to take the right decisions on the management and planning of water resources. As an example, we report here (Figure 8) the hypothetical scenario where maize is irrigated solely by micro-irrigation. It can be useful for critical analysis, localization, and quantitative evaluation of the water savings of potential investments in new micro-irrigation systems. Figure 8 shows that at national level the mean water saving is 21% and in 75% of the cells it goes up up to 28% (59 mm/lgp) In some areas it can have even larger effects: it is evident how the strongest potential water-use reduction of 30-40% is mostly located close to the Alps and the southern Apennines where flow irrigation is now predominant due to the abundance of water (Figure E1(**b**), Appendix E). This information becomes particularly valuable when considering future temperature and precipitation projections. Studies on climate change impacts foresee in the areas close to the mountains an increase in mean temperature of 4°C and a shift of precipitation distribution towards winter periods causing an increase in drought spells in summer [43]. Thus, the increased evapotranspirative water demand caused by the higher temperatures will find even less support in the precipitation water, increasing the stress on the irrigation water.

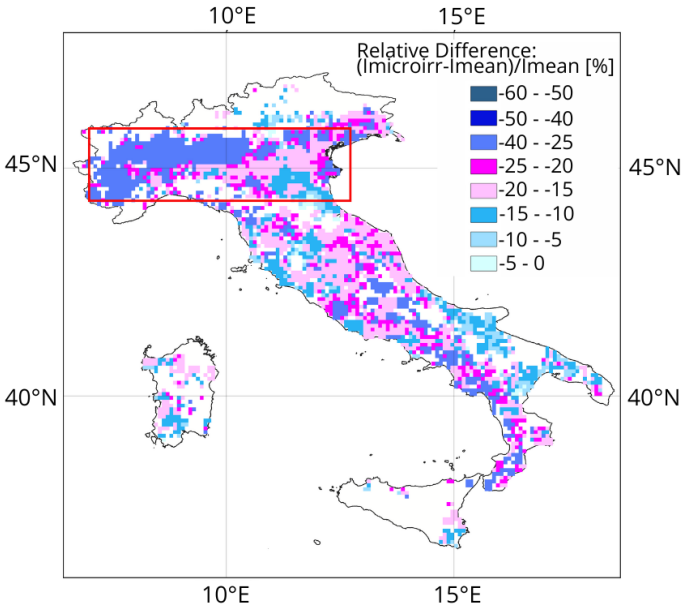

Figure 8. Percentage difference in irrigation water demand when only micro-irrigation is used, compared to the mean irrigation requirement under current mixed irrigation systems.

It is also possible to evaluate how incentives on the increase of micro-irrigation use (where it is already present) can still bring a 5-10% saving. This 5-10% saving becomes of high interest in regions, such as Salentino region (recall the green rectangle in Figure 6(**a**)), very scarce in rain water. Figure 9 shows both the preferred irrigation system (indicated by color) and the amount of water (indicated by shades) currently used in each cell where maize is cultivated. This pair of information allows one to better understand where potential investments would have the greatest impact as it spotlights where large amounts of water are conveyed on the field with inefficient systems. For example, the dark-blue and dark-green areas, corresponding to central regions of Pianura Padana (recall the red rectangle in Figure 6(**a**)), can be identified as key target areas for implementing the most effective changes in irrigation systems: they result the most water-demanding zones and with the most inefficient irrigation systems on ground. At the same time, it is possible to evaluate the feasibility of changing irrigation systems: investments in micro-irrigation are more likely to

be done on fields without existing equipment rather than on areas already equipped with sprinklers.

Table 1. Extension of the areas irrigated with a specific irrigation system in Italy, their efficiencies in Italy [44], and their relative relevance at national scale.

Irrigation system	**Coverage [$10^3 \cdot$ ha]**	**%**	**Efficiency** η
Submersion	221.0	9	0.25
Micro-irrigation	423.0	17	0.9
Flow and Lateral infiltration	748.4	31	0.55
Sprinklers	958.5	40	0.75
Other	68.4	3	0.7

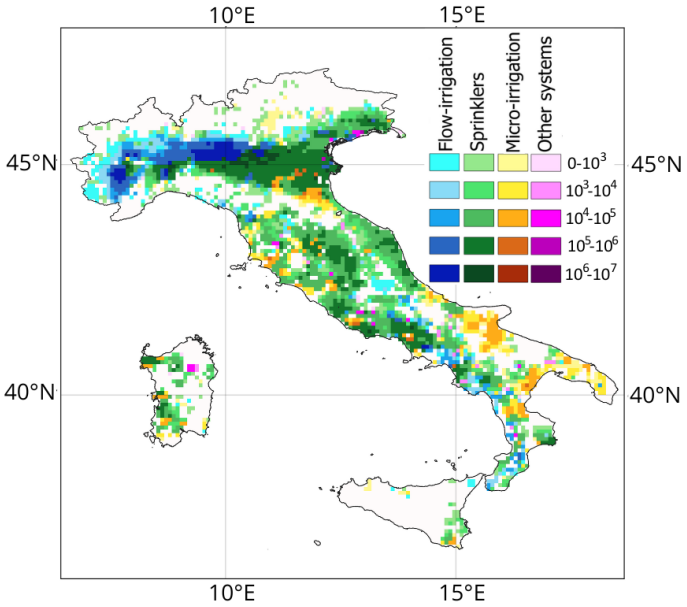

Figure 9. Classification of I_{mz} according to irrigation system (flow irrigation in blue, sprinklers in green, micro irrigation in yellow) and volumetry class (reported to the right of the color legend, in m^3).

In conclusion, the assessment of irrigation demands at regional-national spatial scales and the study of future scenarios are crucial for the correct management and planning of water resources. The agro-hydrological model WaterCropv2 presented here has precisely this purpose and it balances a sufficiently detailed description of physical processes with a manageable data request. Moreover, the model can easily include other information when these are available: e.g. local data on irrigation systems and schedules could be used to reduce uncertainties in the irrigation efficiency assessment.

Appendix E Appendix: data pre-processing

To study the water demand of maize in Italy, accurate research was carried out among databases and literature data to build the best dataset combining availability, accuracy, handiness, and reliability (Table E1). According to the resolution of the selected datasets, the case study was run at 5x5 arc-min (pixel of $\sim$ 8x8 km^2 on average in Italy) cell spatial resolution for the year 2010.

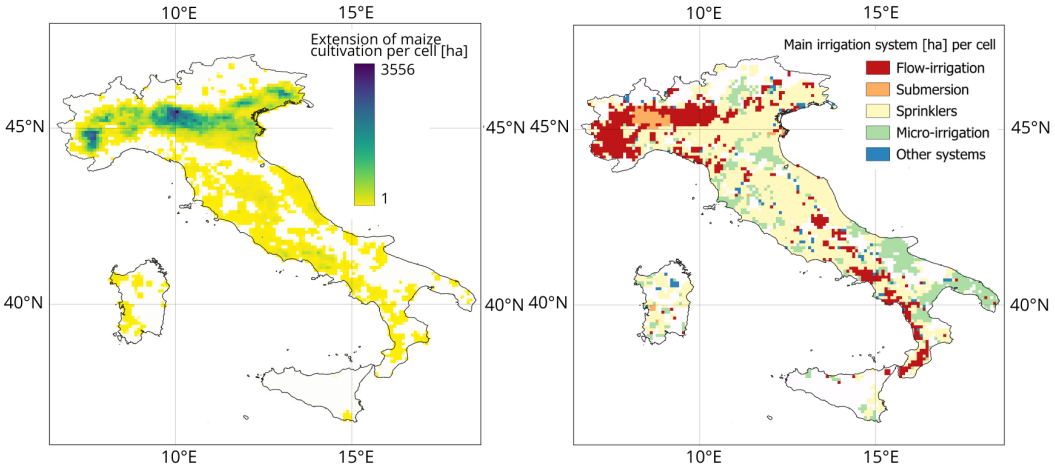

(**a**) (**b**)

Figure E1. Maps of (a) the extension of maize cultivation in each cell, (b) the most extensively adopted irrigation system. Data refer to year 2010.

Table E1. Datasets adopted for the model application to maize in Italy. [1][45],[2][40], [3][46], [4][37], [5][47], [6][48], [7][49], [8], [9][50],[10][44].

Data type	Variable	Dataset	Temporal resolution	Spatial Resolutio
Crop	Potential evapotranspiration	CRU[1]	month	0.5°
	p fraction[3]	-	year	5 arc mi
	$k_c, Dr, Zn_{ini}, Zn_{max}, d_s, d_h$	FAO-56[4]	-	-
Soil	Available water content	Harmonized World [5] Soil Database v1.2	year	5 arc mi
	Pedologic characteristics[6]	-	-	-
	Soil type	LUCAS[7]	year	500 m
Climate	Climate zones	PAMDataset [8]	year	5 arc mi
	Precipitation	ERA5[9]	hour	0.25°
Irrigation	Cultivated areas	CensimentoAgricoltura2010[2]	year	municipal
	Irrigated areas	CensimentoAgricoltura2010[2]	year	municipal
	Irrigation system	CensimentoAgricoltura2010[2]	year	municipal
	Irrigation system efficiency[10]	-	-	-
	Municipalities extensions	ConfiniAmministrativi2010[2]	year	municipal

Crop data. The daily reference evapotranspiration values were defined as 1/30 of the monthly values provided in the CRU dataset [45]. Given the lack of localised characterisation of maize in terms of growth (k_c, Zn_{ini}, Z_{max}) and response to water stress (Dr_*), we referred to general values provided by [51] (Table E2).

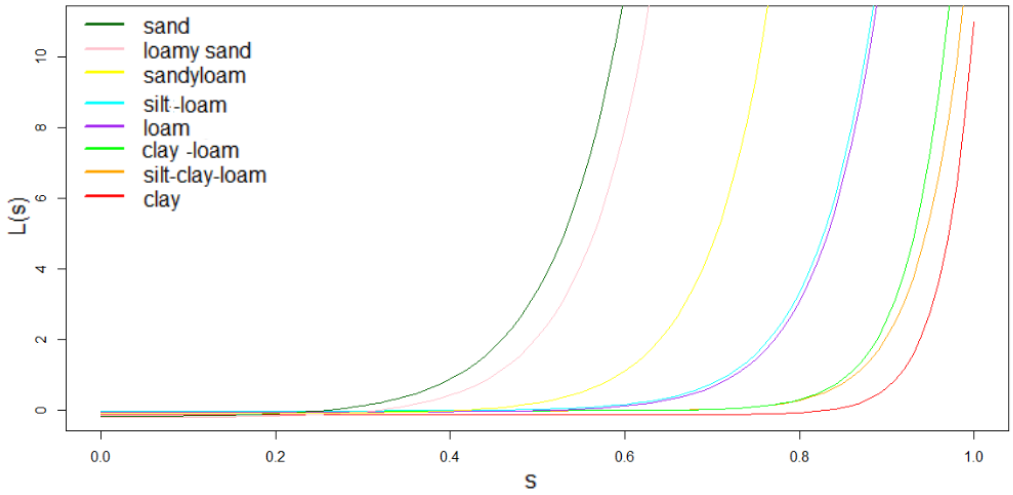

Figure E2. Leakage according to the type of soil. Among the eight soil classes (sand in black, loamy sand in pink, sandy loam in yellow, silt-loam in light blue, loam in purple, clay-loam in green, silt-clay-loam in orange, and clay in red) similar trends to leakage are shown. Thus, the classes were traced back to three: loamy sand (sand and loamy sand), loam (sandy loam, silt-loam and loamy sand) and silt-clay-loam (clay-loam, silt-clay-loam, and clay).

Table E2. Crop parameters for maize [51]

$\mathbf{Zn}_{ini}$	$\mathbf{Zn}_{max}$	$\mathbf{Dr}_{*}$	$\mathbf{kc}_{ini}$	$\mathbf{kc}_{mid}$	$\mathbf{kc}_{end}$
0.3	rf: 1.7 irr: 1	0.55	0.3	1.2	0.5

Differently, the grid dataset of sowing and harvesting dates avaialble for cultivated areas in 2000 [52] allowed us to take into account the quite high climatic heterogeneity of the Italian territory. By employing a resampling process, we were able to define local sowing, d_S, and harvesting dates, d_H. Where cultivated areas existed in 2010 but not in 2000, and consequently lacked corresponding dates, we performed a linear spatial interpolation based on the nearest 24 neighboring cells. Through the evaluation of d_S and d_H, we defined *lgp*: the length of each g-th growing stage. The length of each stage varies according to the climate zone and was computed as a fraction, p, of the total growing period length [46] as

$$lgp_g = p_g \dot{(} d_S - d_H) \tag{E1}$$

Soil data. To categorize the Italian soil in soil classes we relied on the 500 X 500 m resolution dataset LUCAS [49]. As this resolution is higher than 5 arc-min, an upscale was run. The type of soil attributed to the 5 arc-min cell was the most recurring one among the 500 X 500 m cells falling inside the larger cell. To obtain a consistent result, the behavior of the different classes of soil to leakage was compared. The aim was to check whether some classes could be merged into one and, thus, correctly assign a soil type to each 5 arc-min cell. The classes that showed similar trends have pedological differences that can be considered negligible for the aim of this study. Figure E2 shows the different behaviors of the eight soil classes. It is evident how the eight classes group into are four clusters. For the sake of simplicity, even though the sandy-loam class is a cluster on its own, it was associated with loamy sand as very few cells fell in this class, and the remaining classes were traced back to three classes: silt-clay-loam, loam, and loamy-sand.

Typical values of hydraulic soil characteristics, for each class, are reported in Table E3.

Table E3. Soil characteristics [48].

Soil Class	K_s **[mm/h]**	**b**	θ_{sat}	θ_{fc}
Silty-Clay-Loam	0,0612	7,75	0,477	0,275
Loam	0,2502	5,39	0,451	0,225
Loamy sand	5,628	4,38	0,401	0,125

Climate data. Local climate conditions were defined by the climate zones provided in the PAMDataset [47] and the hourly precipitation data were taken from the reanalysis ERA5 dataset [50]. Geographical coordinates correspond to the location of the centroid of each grid cell.

Irrigation data. Data on the extension of irrigated areas were available for 2010, only in listed form and by municipality thanks to the agriculture census ran by the National Institute of Statistics (ISTAT) [40]. To retrieve spatial information (with 5 arc-min resolution) on maize, the listed data were firstly combined with the spatial location of each municipality and, then, rasterized in grid cells (Figure E3). The rasterization was necessary because more than one municipality fell within the same grid cell and each municipality fell within multiple grid cells.

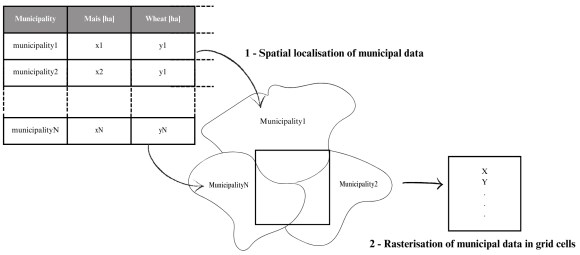

Figure E3. Pre-processing steps to obtain the spatial distribution of irrigated areas. The first step requires to attribute to each municipality, spatially located across Italy, its value of irrigated areas. The second step rasterizes into grid cells the information according to Equation E2.

Lacking details at the sub-municipal scale, we assumed the maize irrigated area of each municipality ha_m to be homogeneously distributed within each municipality m. Hence, for each grid cell, c, the maize irrigated area ha_c [ha] was computed assuming that (i) the percentage of the municipality extension within the grid cell could be directly applied to the irrigated area, (ii) ha_c to be homogeneously distributed within the grid cell, and (iii) ha_c to be defined as the sum of the percentages of irrigated areas of the *m-tot* municipalities that fell within the grid cell. It follows:

$$ha_c = \sum_{m=1}^{m-tot} ha_m \frac{A_{m,c}}{A_m} \tag{E2}$$

where ha_m stands for the maize irrigated area within the m-th municipality, A_m for the municipality area, $A_{m,c}$ for the municipality extent within the grid cell.

Unfortunately, the CensimentoAgricoltura2010 database provides, for each crop and municipality, data on the amount of irrigated hectares but not the specific irrigation system used for each crop. This did not allow us to define a local maize-specific value for the inefficiency factor α.

To overcome this gap, information about the typical irrigation systems used for maize in each cell was intersected with information on the available irrigation systems in each municipality. It was thus possible to define, for each cell, a plausible mix of used irrigation systems. Typically, in Italy, maize is irrigated with flow and lateral infiltration, sprinklers,

and micro-irrigation systems and for their efficiencies we referred to data published by the Italian Ministry of Agriculture Food Sovereignty and Forestry [44] reported in table 1.

Hence, for each cell, c, the inefficiency factor α was computed as

$$\alpha_c = \sum_y \left(\frac{1}{\eta_y} \frac{ha_y}{ha_{tot}}\right) \tag{E3}$$

where y stands for each irrigation system used in the cell, η_y for the corresponding efficiency, ha_y for the hectares irrigated with the irrigation system y, and ha_{tot} for the total amount of irrigated hectares within the cell.

Appendix F Appendix: trends of roots growth, crop and stress coefficient

Figure F1 reports the trends of Zn and k_c during the growing stages of the growing season. Figure F2, instead, shows the trend of k_s as function of the soil water content WC.

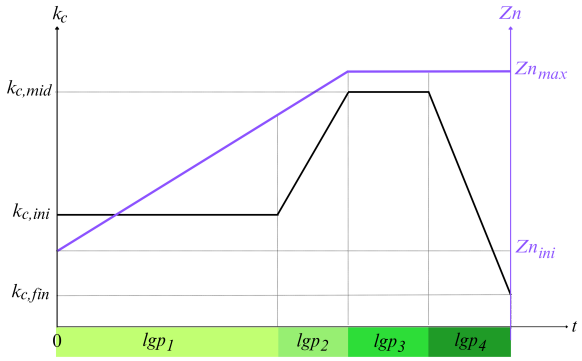

Figure F1. Qualitative description of the crop coefficient k_c (in black) and the elongation of the roots Zn (in purple) during the growing stages lgps of the growing season.

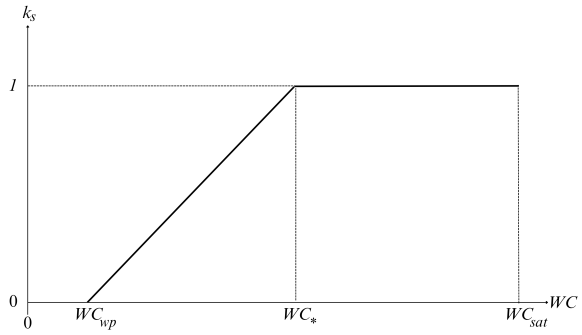

Figure F2. Qualitative description of the crop coefficient, k_s, according to the soil water content.

Conflict of Interest

The authors declare no conflicts of interest relevant to this study.

Data Availability Statement

The data analysis was performed using [53]. The R scripts and the data used to execute the analyses in the paper can be found at [**?**]

Acknowledgments

This study was carried out within the "National Research Centre for Agricultural Technologies – AGRITECH" and received funding from the European Union Next-GenerationEU (PIANO NAZIONALE DI RIPRESA E RESILIENZA (PNRR) – MISSIONE

4 COMPONENTE 2, INVESTIMENTO 1.4 – Avviso n. 3138 del 16/12/2021, Codice Programma CN00000022). This manuscript reflects only the authors' views and opinions, neither the European Union nor the European Commission can be considered responsible for them.

1. Rudebeck, T. Introducing Corporate Water Stewardship in the Context of Global Water Governance. In: Water Governance - Concepts, Methods, and Practice. *Springer* **2019**. https://doi.org/https://doi.org/10.1007/978-3-030-13225-5_1.
2. Biswas, A.K.; Tortajada, C. Future Water Governance: Problems and Perspectives. *Water Resources Development* **2010**, *26*, 129–139. https://doi.org/10.1080/07900627.2010.488853.
3. FAO. Water auditing/water governance analysis – Governance and policy support: Methodological framework **2024**. https://doi.org/https://doi.org/10.4060/cc8993en.
4. Cherlet, M.; Hutchinson, C.; Reynolds, J.; Hill, J.; Sommer, S.; von Maltitz (Eds.), G. World Atlas of Desertification - Increasing Production. *Publication Office of the European Union* **2018**. https://doi.org/10.2760/06292.
5. Wu, B.; Tian, F.; Zhang, M.; Piao, S.; Zeng, H.; Zhu, W.; Liu, J.; .; Elnashar, A.; Lu, Y. Quantifying global agricultural water appropriation with data derived from earth observations. *Journal of Cleaner Production* **2022**, *358*. https://doi.org/https://doi.org/10.1016/j.jclepro.2022.131891.
6. FAO. *The state of the world's land and water resources for food and agriculture (SOLAW) - Managing systems at risk.*; Food and Agriculture Organization of the United Nations, 2011.
7. Fujs, T.; Kashiwase, H. Strains on freshwater resources: The impact of food production on water consumption. *World Bank - Data Blog* **2023**.
8. Godfray, H.C.J.; Beddington, J.R.; Crute, I.R.; Haddad, L.; Lawrence, D.; Muir, J.F.; Pretty, J.; Robinson, S.; Thomas, S.M.; Toulmin, C. Food security: the challenge of feeding 9 billion people. *Science* **2010**, *327*, 812–818. https://doi.org/10.1126/science.1185383.
9. Wallace, J. Increasing agricultural water use efficiency to meet future food production. *Agriculture, Ecosystems and Environment* **2000**, *82*, 105–119. https://doi.org/https://doi.org/10.1016/S0167-8809(00)00220-6.
10. Pfister, S.; Bayer, P.; Koehler, A.; Hellweg, S. Projected water consumption in future global agriculture: Scenarios and related impacts. *Science of The Total Environment* **2011**, *409*, 4206–4216. https://doi.org/https://doi.org/10.1016/j.scitotenv.2011.07.019.
11. Vogel, E.; Donat, M.G.; Alexander, L.V.; Meinshausen, M.; Ray, D.K.; Karoly, D.; Meinshausen, N.; Frieler, K. The effects of climate extremes on global agricultural yields. *Environ. Res. Lett.* **2019**, *14*. https://doi.org/10.1088/1748-9326/ab154b.
12. Kundzewicz, Z.W. Climate change impacts on the hydrological cycle. *Ecohydrology Hydrobiology* **2008**, *8*, 195–203. https://doi.org/https://doi.org/10.2478/v10104-009-0015-y.
13. Stagl, J.; Mayr, E.; Koch, H.; Hattermann., F.; Huang, S. Effects of Climate Change on the Hydrological Cycle in Central and Eastern Europe. In: Rannow, S., Neubert, M. (eds) Managing Protected Areas in Central and Eastern Europe Under Climate Change. *Advances in Global Change Research* **2014**, *58*. https://doi.org/https://doi.org/10.1007/978-94-007-7960-0_3.
14. Ma, J.; Zhou, L.; Foltz, G.R.; Qu, X.; Ying, J.; Tokinaga, H.; Mechoso, C.R.; Li, J.; Gu, X. Hydrological cycle changes under global warming and their effects on multiscale climate variability. *Annals of the New York Academy of Science. Special Issue: The Year in Climate Science Research* **2020**, pp. 1–172. https://doi.org/https://doi.org/10.1111/nyas.14335.
15. X., W.; L., L. The Impacts of Climate Change on the Hydrological Cycle and Water Resource Management. *Water* **2019**, *15*. https://doi.org/https://doi.org/10.3390/w15132342.
16. Peters-Lidard, C.D.; Rose, K.C.; Kiang, J.E.; Strobel, M.L.; Anderson, M.L.; Byrd, A.R.; Kolian, M.J.; Brekke, L.D.; Arndt, D.S. Indicators of climate change impacts on the water cycle and water management. *Climatic Change* **2021**, *165*. https://doi.org/https://doi.org/10.1007/s10584-021-03057-5.
17. Wriedt, G.; der Velde, M.V.; Aloe, A.; Bouraoui, F. Estimating irrigation water requirements in Europe. *Journal of Hydrology* **2009**, *373*, 527–544. https://doi.org/https://doi.org/10.1016/j.jhydrol.2009.05.018.

18. FAO.; OECD. The assessment of climate change-related vulnerability in the agricultural sector: reviewing conceptual frameworks **2012**. https://doi.org/10.13140/2.1.4314.8809.
19. EUCAP-Network. Agricultural Rural Inspiration Awards (ARIA). *EU CAP Network* **2023**.
20. EUCAP-Network. Water efficiency benefits flow from CAP Strategic Plans. *EU CAP Network* **2024**, pp. 1–172.
21. Hayashi, A.; Akimoto, K.; Tomoda, T.; Kii, M. Global evaluation of the effects of agriculture and water management adaptations on the water-stressed population. *Mitig Adapt Strateg Glob Change* **2013**, *18*, 591–618. https://doi.org/https://doi.org/10.1007/s11027-012-9377-3.
22. Pereira, L.S. Agriculture and Food: Challenges and Issues. *Water Resour Manage* **2017**, *31*, 2985–2999. https://doi.org/https://doi.org/10.1007/s11269-017-1664-z.
23. Díaz, J.A.R.; Perea, R.G.; Ángel Moreno, M. Modelling and Management of Irrigation System. *Water* **2020**, *12*. https://doi.org/https://doi.org/10.3390/w12030697.
24. Maton, L.; Leenhardt, D.; Goulard, M.; Bergez, J.E. Assessing the irrigation strategies over a wide geographical area from structural data about farming systems. *Agricultural Systems* **2005**, *86*, 293–311. https://doi.org/https://doi.org/10.1016/j.agsy.2004.09.010.
25. Cancela, J.; Cuesta, T.; Neira, X.; Pereira, L. Modelling for Improved Irrigation Water Management in a Temperate Region of Northern Spain. *Biosystems Engineering* **2006**, *94*, 151–163. https://doi.org/10.1016/J.BIOSYSTEMSENG.2006.02.010.
26. Singh, A. Irrigation Planning and Management Through Optimization Modelling. *Water Resources Management* **2014**, *28*, 1–14. https://doi.org/https://doi.org/10.1007/s11269-013-0469-y.
27. Olivera-Guerra, L.E.; Laluet, P.; Altés, V.; Ollivier, C.; Pageot, Y.; Paolini, G.; Chavanon, E.; Rivalland, V.; Boulet, G.; Villar, J.M.; et al. Modeling actual water use under different irrigation regimes at district scale: Application to the FAO-56 dual crop coefficient method. *Agricultural Water Management* **2023**, *278*. https://doi.org/https://doi.org/10.1016/j.agwat.2022.108119.
28. Bastiaanssen, W.; Allen, R.; Droogers, P.; D'Urso, G.; Steduto, P. Twenty-five years modeling irrigated and drained soils: State of the art. *Agricultural Water Management* **2007**, *92*, 111–125. https://doi.org/10.1016/j.agwat.2007.05.013.
29. Lazarovitch, N.; Kisekka, I.; .; Oker, T.E.; Brunetti, G.; .; Wöhling, T.; Xianyue, L.; Yong, L.; Skaggs, T.H.; et al. Chapter Two - Modeling of irrigation and related processes with HYDRUS. *Advances in Agronomy* **2023**, *181*, 79–181. https://doi.org/https://doi.org/10.1016/bs.agron.2023.05.002.
30. Schaphoff, S.; von Bloh, W.; Rammig, A.; Thonicke, K.; Biemans, H.; Forkel, M.; Gerten, D.; Heinke, J.; Jägermeyr, J.; Knauer, J.; et al. LPJmL4 – a dynamic global vegetation model with managed land – Part 1: Model description. *Geosci. Model Dev.* **2018**, *11*, 1343–1375. https://doi.org/https://doi.org/10.5194/gmd-11-1343-2018.
31. Knox, J.; Weatherhead, E.; Bradley, R. Mapping the spatial distribution of volumetric irrigation water requirements for maincrop potatoes in England and Wales. *Agricultural Water Management* **1996**, *31*, 1–15. https://doi.org/https://doi.org/10.1016/0378-3774(96)01238-3.
32. Mohammadi, N.K. A Review on GIS in Irrigation and Water Management. *International Journal of Engineering Research Technology* **2019**, *8*.
33. Hanasaki, N.; Yoshikawa, S.; Pokhrel, Y.; Kanae, S. A global hydrological simulation to specify the sources of water used by humans. *Hydrol. Earth Syst. Sci.* **2018**, *22*, 789–817. https://doi.org/https://doi.org/10.5194/hess-22-789-2018.
34. Chiarelli, D.D.; Passera, C.; Rosa, L.; Davis, K.F.; D'Odorico, P.; Rulli, M.C. The green and blue crop water requirement WATNEEDS model and its global gridded outputs. *Sci Data* **2020**, *7*. https://doi.org/https://doi.org/10.1038/s41597-020-00612-0.
35. Doell, P.; Siebert, S. Global modeling of irrigation water requirements. *Water Resources Research* **2002**, *38*. https://doi.org/10.1029/2001wr000355.
36. Tuninetti, M.; Tamea, S.; D'Odorico, P.; Laio, F.; Ridolfi, L. Global sensitivity of high-resolution estimates of crop water footprint. *Water Resources Research* **2015**, *51*, 8257–8272. https://doi.org/10.1002/2015WR017148.
37. Allen, R.; Pereira, L.; Raes, D.; Smith, M. Crop evapotranspiration - Guidelines for computing crop water requirements - FAO Irrigation and drainage paper 56. *FAO - Food and Agiculture Organization of the United Nations* **1998**.

38. Jackson, R.D.; Hatfield, J.L.; Reginato, R.J.; Idso, S.B.; Pinter, P.J.J. Estimation of daily evapotranspiration from one-time-of-day measurements. *Agric. Water Manage.* **1983**, *7(3)*, 351–362. https://doi.org/10.1016/0378-3774(83)90095-1.
39. Laio, F.; Porporato, A.; Ridolfi, L.; Rodriguez-Iturbe, I. Plants in water-controlled ecosystems: active role in hydrologic processes and responce to water stress II. Probabilistic soil moisture dynamics. *Advances in Water Research* **2002**, *24*, 707–723. https://doi.org/https://doi.org/10.1016/S0309-1708(01)00005-7.
40. ISTAT. $6^{i}h$ General Agricultural Census: Use of water resources for irrigation purpuses in agriculture (6° Censimento Generale dell'Agricoltura: UTILIZZO DELLA RISORSA IDRICA A FINI IRRIGUI IN AGRICOLTURA). *STEALTH* **2014**.
41. Lupia, F.; Vanino, S.; Santis, F.D.; Laruccia, N. A model-based irrigation water consumption estimation at farm level. *INEA* **2013**.
42. ISPRA. Indicators of Italian climate in 2020 (Gli indicatori del clima in Italia del 2020) **2021**.
43. Coppola, E.; Giorgi, F. An assessment of temperature and precipitation change projections over Italy from recent global and regional climate model simulations. *Int. J. Climatol* **2010**, *30*, 11–32. https://doi.org/10.1002/joc.1867.
44. MIPAAF. Metodologia di stima degli utilizzi e delle restituzioni. Technical report, Ministry of Agriculture, Food Sovereignty and Forestry, 2016.
45. Harris, I.; Osborn, T.; Jones, P.; Lister, D. Version 4 of the CRU TS monthly high-resolution gridded multivariate climate dataset. *Sci. Data* **2020**, *7*, 1–18. https://doi.org/https://doi.org/10.1038/s41597-020-0453-3.
46. Mekonnen, M.M.; Hoekstra, A.Y. The green, blue and grey water footprint of crops and derived crop products. *Hydrol. Earth Syst. Sci.* **2011**, *15*, 1577–1600. https://doi.org/10.5194/hess-15-1577-2011.
47. Fischer, G.; Nachtergaele, F.; Prieler, S.; van Velthuizen, H.; Verelst, L.; Wiberg, D. Global Agro-ecological Zones Assessment for Agriculture. *IIASA* **2008**.
48. Clapp, R.; Hornberger, G. Empirical Equations for Some Soil Hydraulic Properties. *Water Resources Research* **1978**, *14*, 601–604. https://doi.org/https://doi.org/10.1029/WR014i004p00601.
49. Ballabio, C.; Panagos, P.; Monatanarella, L. Mapping topsoil physical properties at European scale using the LUCAS database. *Geoderma* **2016**, *261*, 110–123. https://doi.org/https://doi.org/10.1016/j.geoderma.2015.07.006.
50. Hersbach, H.; Bell, B.; Berrisford, P.; Biavati, G.; Horányi, A.; Sabater, J.M.; Nicolas, J.; Peubey, C.; Radu, R.; Rozum, I.; et al. ERA5 hourly data on single levels from 1940 to present. *Copernicus Climate Change Service (C3S)* **2023**. https://doi.org/10.24381/cds.adbb2d47.
51. Pereira, L.; Paredes, P.; Melton, F.; Johnson, L.; Wang, T.; López-Urrea, R.; Cancela, J.; Allen, R. Prediction of crop coefficients from fraction of ground cover and height. Background and validation using ground and remote sensing data. *Agricultural Waer Management* **2020**, *241*. https://doi.org/https://doi.org/10.1016/j.agwat.2020.106197.
52. Portmann, F.; Siebert, S.; Döll, P. MIRCA2000—Global monthly irrigated and rainfed crop areas around the year 2000: A new high-resolution data set for agricultural and hydrological modeling. *Global Biogeochemical Cycles* **2010**, *24*. https://doi.org/10.1029/2008GB003435.
53. R Core Team. *R: A Language and Environment for Statistical Computing*. R Foundation for Statistical Computing, Vienna, Austria, 2021.